Science Arts & Métiers (SAM)

is an open access repository that collects the work of Arts et Métiers Institute of Technology researchers and makes it freely available over the web where possible.

This is an author-deposited version published in: https://sam.ensam.eu
Handle ID: .http://hdl.handle.net/10985/19996

To cite this version :

M. A. LARIBI, R. TIEBI, S. TAMBOURA, Mohammadali SHIRINBAYAN, Abbas TCHARKHTCHI, Joseph FITOUSSI - Sheet Molding Compound Automotive Component Reliability Using a Micromechanical Damage Approach - Applied Composite Materials - Vol. 27, p.693-715 - 2020

Any correspondence concerning this service should be sent to the repository Administrator : scienceouverte@ensam.eu

Arts et Métiers Institute of Technology

Sheet Molding Compound Automotive Component Reliability Using a Micromechanical Damage Approach

M. A. Laribi[1,2] · R. TieBi[3] · S. Tamboura[4] · M. Shirinbayan[1] · A. Tcharkhtchi[1] · H. Ben Dali[4] · J. Fitoussi[1]

Abstract
The mastering of product reliability is essential for industrial competitiveness. If for metallic materials the topic is well-known, especially in automotive industry, Original Equipment Manufacturers are expecting strong support of their suppliers to full-fill the lack data. This paper presents a new original approach, using a micromechanical based on damage model to address the problem of reliability of Sheet Molding Compound (SMC) components. The first part demonstrates the inadequacy of the standard method of reliability on SMC material through its application on the new Peugeot 3008. In fact, the very flat S-N curve of SMC, and in general, composite materials is not appropriate for acceleration effect. The proposed model correlates the stress, damage and strength with both cycle number and slamming velocity. It emphasizes the relation between the effective distribution with the slamming velocity effect. Then, a new reliability approach based on a micromechanical fatigue/damage model was developed. The definition of new probability distributions based on damage was necessary to apply properly the stress-resistance approach. It allows taking into account the velocity effect by switching in damage space. Finally, applying this new methodology on the Peugeot 3008, leads to the definition of the optimal validation laboratory tests to ensure the reliability. Indeed, the required number of cycles to ensure reliability has been reduced significantly. Micromechanical damage reliability approach could be an efficient way to ensure the reliability of short fiber reinforcement composite components used in industrial context.

Keywords Reliability · Damage · Automotive · Composites · SMC

1 Introduction

Fiber-reinforced composite materials applications were initially mostly associated to aerospace and marine industries. In fact, their exceptional mechanical properties made them very

✉ M. A. Laribi
mohamed–amine.laribi@iut–tlse3.fr

attractive in many engineering fields. However, their manufacturing processes and their heterogeneous nature open the door for many geometric and physical uncertainties at all scales [1]. Thus, important factors of safety are still introduced to ensure reliability and to cover the stronger dispersion of their mechanical properties [2, 3]. In fact, in structural engineering, reliability is considered to be one of the most commonly used indicators for interpreting response information for design, repair, maintenance, etc. Over the past decades, many authors contributed to the understanding of reliability and probabilistic failure of composites. [4–6]. To avoid using such a height safety factors, it is very important to identify and quantify the effect of these uncertainties at their real scale (occurrence scale) and then propagate their effect at the composite component scale. However, multi-scale modelling approach are ideal tools for linking micro-scale parameters to macro-scale parameters and for propagating micro-scale to macro-scale uncertainties [7, 8]. Consequently, this could lead to efficient design and safer use of composites.

In real automotive composites structures, such as a conveyor belt [9], a subfloor structure [10], a windscreen contour [11] or a suspension arm [12] composite microstructures are always determined by the forming process. For Sheet Molding Compound (SMC) composite materials, automotive components are generally produced by a compression process of preimpregnated fibre sheets which frequently involves a high flow of material during molding. The material flow during treatment induces fibre orientation distributions strongly affected by mould geometry [13, 14]. Consequently, real SMC composites structures contain multiple microstructures that are extremely variable from one place to another. Therefore, real composite structures always exhibit high spatial variation in mechanical properties. That's why, for an efficient structural design, the knowledge of the spatial distribution of microstructure is a crucial need. Consequently, an accurate prediction of anisotropic, process-dependent and inhomogeneous mechanical properties can help reduce costly prototyping and further reduce development cycles.

In automotive industry, car manufacturers are demanding of their suppliers to manage the reliability topic in order to set-up the appropriate validation laboratory tests. This requirement becomes even more critical especially for plastic/composite components such as tailgate, spare wheel tray, front end carrier or floor when safety is involved. The specification of PSA (Peugeot Société Anonyme) [15], during the designing phase of the new Peugeot 3008, was based on previous metallic components, whereas this component is made of Sheet Molding Compound (SMC) material. To ensure its reliability during the development phase, we suggest in this paper to introduce the damage/fatigue specific behaviour of SMC. Thus, this study was the key element for an original and useful approach of reliability.

First of all, the inadequacy of the standard method of reliability extrapolated from steel material [16, 17], will be highlighted.

The second part of the paper presents a new fatigue damage approach based on Laribi & al. [18] previous study dealing with SMC materials. The model was adapted to build a pragmatic but rigorous approach used to ensure the design of the Peugeot 3008 tailgate component.

The third part describes the main idea of the new approach based on the damage law. From the given probabilities of the number of cycles and the tailgate slamming velocity, a new distribution of stress will is presented. The identification of the ETA (η) parameter of the Weibull resistance law is illustrated, using the stress-resistance method.

Finally, the application on the new Peugeot 3008 will be presented. It will show how to define the proper laboratory tests to validate the reliability of the tailgate component.

2 Standard Reliability Method

2.1 Problematic

The key question in the reliability problematic is to define the minimal representative laboratory tests in order to ensure the robustness at end customer level. The main required data necessary to set-up and solve the problem of the reliability are [15, 19]:

- The admissible level of *ppm* (part per million)
- The confidence level (in percentage). Depending on the criticality of the event, the confidence level can vary from *50%* to *90%*.
- The distribution law of the stress which is generally given as common probabilities laws (Normal, LogNormal, Weibull, etc.).
- The distribution law of the resistance which is commonly also a statistic law.
- The choice of the number of samples to pass the laboratory test to validate the component reliability target.

2.2 Loading at Constant Stress Level

In the standard reliability method [16, 17, 19], the stress-resistance method is applied to identify the resistance law parameters. Then, the final number of cycle can be easily calculated with the given confidence percentage value and the number of successful tests. It is usual to consider the Wohler S-N curves to perform the acceleration method in order to reduce the number of cycle to be applied in the validation stage. The temperature effect can also be taken into account, coupled or not with the stress effect. This paragraph describes step by step the application of this approach on the new Peugeot 3008 tailgate reinforced with SMC material.

To preserve the confidentiality of the data provided by PSA, the law parameters and the results will be normalized most of the time without affecting the coherence of the resulting deductions.

The main data obtained from PSA [15] are listed below:

- Part per million *(ppm)* for a given number of years
- Confidence level
- The stress distribution is represented by a LogNormal law which mean and standard deviation are respectively $\mu logn$ and $\sigma logn$. The stress distribution can be expressed by [19, 20]:

$$g(N) = \frac{1}{N.\sigma logn.\sqrt{2\pi}} e^{-\frac{1}{2}\left(\frac{(ln(N)-\mu logn)}{\sigma logn}\right)^2} \quad (1)$$

where N is the number of applied cycles. It represents how often the tailgate will be slammed during the vehicle lifetime.

Using experimental data, the parameters of the component behaviour dispersion law has been identified in the Weibull form defined below [19, 20]:

$$f(N) = \frac{\beta}{\eta}\left(\frac{N-\gamma}{\eta}\right)^{\beta-1} e^{-\left(\frac{N-\gamma}{\eta}\right)^{\beta}} \tag{2}$$

where N is the number of slamming cycles of the tailgate and β, γ and η are the parameters of Weibull law distribution.

Note that $\gamma > 0$, indicates that default can occur inside the component during its production phase. In our present case it is assumed that damage starts only after production during customer use of the car: Consequently, $\gamma = 0$ can be assumed leading to the modified expression of Eq. (2):

$$f(N) = \frac{\beta}{\eta}\left(\frac{N}{\eta}\right)^{\beta-1} e^{-\left(\frac{N}{\eta}\right)^{\beta}} \tag{3}$$

The parameter Beta (β) was identified from tensile tests performed on specimens cut from laboratory plates. Other tests are planned on the intermediate part and also on the global tailgate perimeter in order to confirm or to correct β identified value. To identify the (η) parameter, we have applied the stress-resistance method which principle is illustrated in Fig. 1.

The elementary *ppm* (Δppm) due to the loading at *Ns* cycles, is the product of the elementary stress probability *g(Ns)dNs* and the failure probability of the resistance until the *Ns* cycle. Its expression is given below [19, 20]:

$$\Delta(ppm) = [g(Ns)dNs] \int_0^{Ns} f(Nr)dNr \tag{4}$$

If *F(Nr)* is the cumulative function of the resistance, the rate of *ppm* becomes:

$$\Delta(ppm) = [g(Ns)dNs]F(Ns) \tag{5}$$

Finally the global *ppm* is easily obtained from the following integral form:

$$ppm = \int_0^{+\infty} [g(Ns)F(Ns)]dNs \tag{6}$$

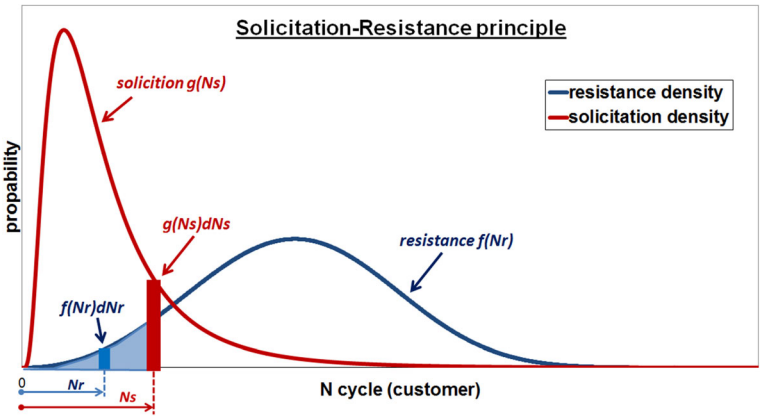

Fig. 1 Method of stress-resistance, principle

The cumulative form of the Weibull resistance function is given by:

$$F(N) = 1 - e^{-\left(\frac{N}{\eta}\right)^{\beta}} \tag{7}$$

2.3 Application on the New 3008 Tailgate

The integral Eq. (6) was solved by using a Python solver and the parameter η of the Weibull law was identified. The normalized value is $\eta = 400{,}000\ cycles$.

To reach the final number of validation cycles, it's necessary to define the number of successful tests (*nst*). AEE has chosen $nst = 6$ tests in agreement with PSA. With the given confidence level (1-risk) and according to the binomial law (Bernoulli test), the final cycle number was calculated. The binomial law is remembered by the Eq. (8).

$$P(X \leq k) = \sum_{k=0}^{nst} \binom{k}{nst} p^k (1-p)^{nst-k} \tag{8}$$

$P(X \leq k)$ is the probability of the random variable X. It represents the acceptable risk. k is the number of failed tests (here k must be equal to *zero*). From this hypothesis, the target probability p and the final number of cycles were determined. We have obtained $Ncycle = 240{,}000\ (normalized\ value)$.

The graph on the previous Fig. 2 in the Weibull Log/Log space can illustrate this result.

2.4 Stress Acceleration

In order to reduce the minimum required number of cycles for validation, the stress was "accelerated" by increasing the slamming velocity. Structural simulation by FEM tools was performed on the tailgate. The results extracted on the most critical areas (Fig. 3) are plotted on the graphs of Fig. 4.

From FEM result, the relationship between slamming velocity and internal stress was established and described by a fourth-order polynomial function between *0.25 m/s* and *2.5 m/s*.

In addition to the FEM analysis, fatigue tests on tensile specimens were performed [18]. The effect of fibre orientation was studied. However, for the sake of simplification, this paper

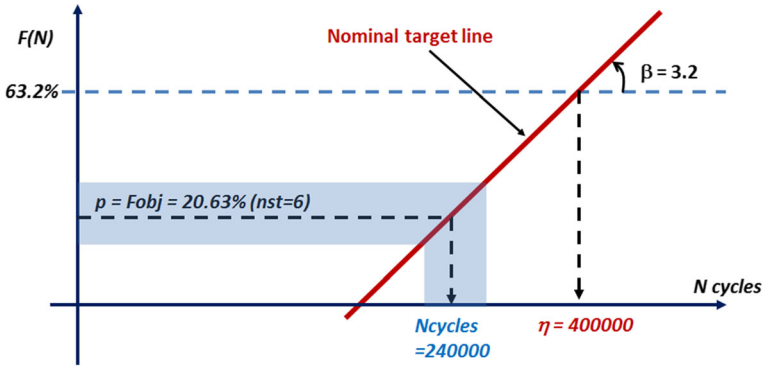

Fig. 2 Log/Log representation of the S-R solution

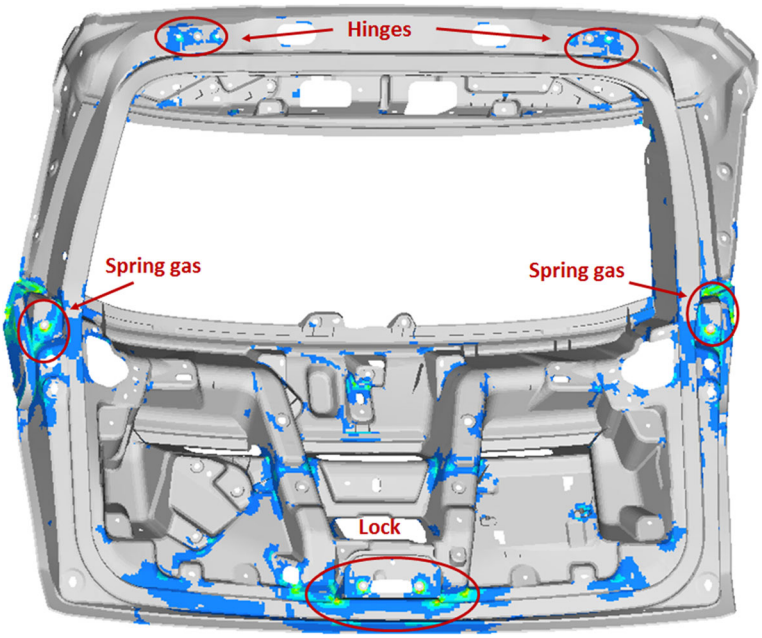

Fig. 3 Stress/slamming velocity by FEM analysis

is focused on quasi-isotropic behaviour of the SMC (due to the quasi-full loading of the mold). The following figure shows the Wohler S-N curves extracted from fatigue tests.

One can note the high sensitivity of the fatigue behaviour of this SMC material. A variation of only *5 MPa* can produce a variation of *100,000* cycles on fatigue life. From these curves, Basquin coefficients have been identified for each flowing configuration. The Basquin slope

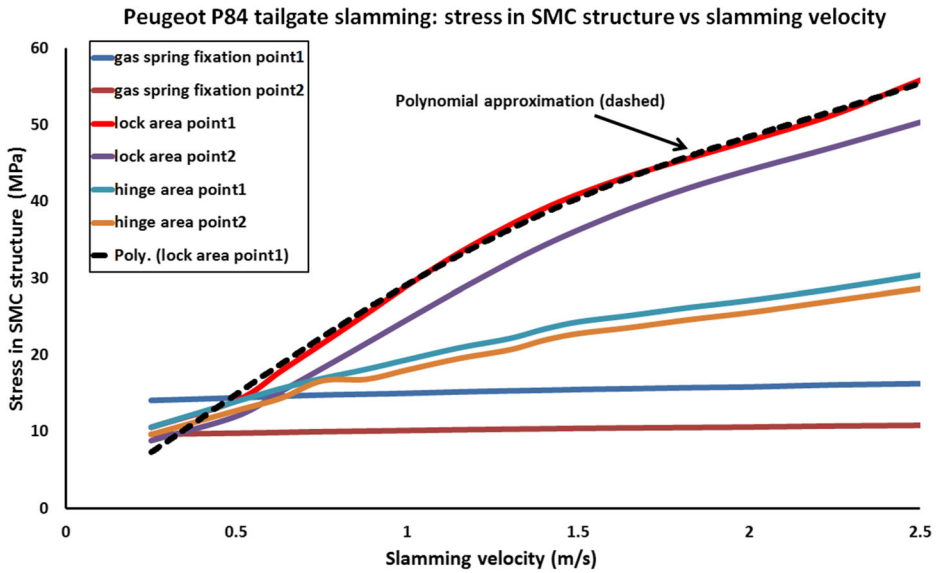

Fig. 4 Stress/slamming velocity by FEM analysis

varies from *20* at longitudinal direction to *67* in transverse direction. It is about *76.9* for the no flowed direction (quasi-isotropic).

This very specific fatigue behaviour of composite material was confirmed by other studies performed on glass fibres reinforced thermoplastics. Compared to steel, S-N curves of short fibres reinforced composites are generally very flat.

Using the identified SMC Basquin law, and taking into account the relationship between internal stress and tailgate slamming velocity, the accelerated cycle number has been calculated. In this approach, one may consider the following definitions:

- The reference slamming velocity is noted V_{ref}. The stress due to this velocity is σ_{ref}.
- The accelerated slamming velocity will be noted V_{acc} and σ_{acc} its corresponding internal stress.
- We will note k the acceleration factor:

$$k = \frac{\sigma_{acc}}{\sigma_{ref}} \tag{9}$$

For the validation physical test recommended by PSA, the acceleration factor was about $k = 1.35$. The corresponding accelerated number of cycles N_{acc} can be expressed as:

$$N_{acc} = N_{ref} * k^{-76.9} = 0.000022\ cycle \tag{10}$$

where $N_{ref} = 240{,}000$ is the reference number of cycles obtained at the slamming velocity V_{ref}.

2.5 Discussion

The accelerated number of cycle obtained ($2.2e^{-5}$) by using the standard approach based on the Basquin law, is obviously unrealistic. The very high sensitivity of the material behaviour (Fig. 5) prevents from taking into account stress effect. A numerical issue is reached immediately when applying the stress variation from the reference value. In fact, the velocity at the end

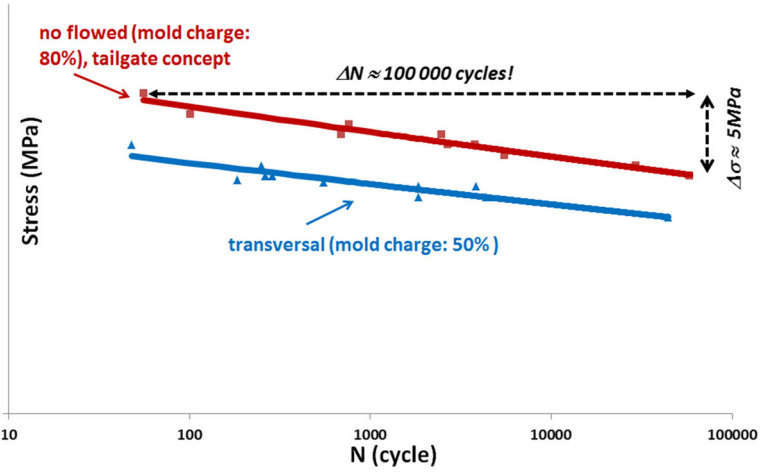

Fig. 5 SMC S-N curve with fibre orientation effect

customer is not constant. Figure 6 briefly presents the dispersion as a Normal law, provided by PSA.

The Basquin law approach assumes also the linearity of the damage until final failure. This is in contradiction with the experimental observations.

So, the necessity of a new approach is mandatory to solve the problem of the reliability of composites material such as SMC. Before the presentation of this approach, the damage model is briefly presented in the next chapter.

3 SMC Damage/Fatigue Constitutive Law

3.1 Previous Work

Several studies have been conducted concerning the mechanical behaviour of several SMC composites formulations [13, 21–25]. The focus has been on the multi-scale experimental analysis and modelling of the mechanical behaviour and damage of this class of composites materials [27, 28]. It has been demonstrated that the non-linear behaviour of a standard SMC (such as the one in study) is mainly governed by fibre-matrix interface failure [21–23]. Accumulation and propagation of local damage during fatigue loading lead to a progressive loss of stiffness during fatigue loading [22]. Final failure appears when the micro-cracks density reaches a certain critical value. Then, a pseudo-delamination phenomenon takes place just before final failure. Therefore, it is obvious that a fatigue life prediction model for SMC composites should be based on a micromechanical approach taking into account the damage phenomenon at the local scale. Thus, continuous efforts have been dedicated to the multi-scale modelling of short fibres reinforced composites submitted to quasi-static [21, 23], high strain rate [26] and fatigue behaviour [22, 24]. However, computing times using this kind of approach for fatigue modelling are often too long and not suitable for real composite automotive components. On the other hand, phenomenological approaches are not enough appropriate for these highly heterogeneous materials presenting complex microstructures and cannot describe properly the effect of microstructure on damage development.

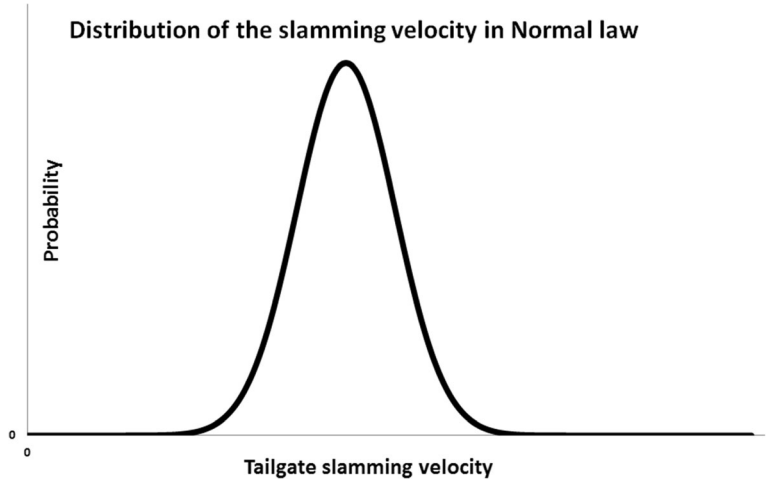

Fig. 6 Tailgate slamming velocity distribution

In this study, we used a hybrid approach [18] which combines a micromechanical approach with a phenomenological one. The originality of this methodology lies in using the outputs of a micromechanical damage model identified in a simple tensile configuration into a phenomenological formulation of the fatigue loss of stiffness. Fiber-matrix interface decohesion is known to be a main local damage mechanism in SMC composites (see Fig. 7). This phenomenon is introduced in the Mori and Tanaka approach through a local damage criterion which defines step by step the number of micro-cracks to be introduced in the homogenization scheme of Mori and Tanaka during loading until final failure.

At each calculation step, the Mori and Tanaka model is used to predict the evolution of the relative stiffness E/E_0 as a function of the micro-cracks density progressively introduced using the local damage criterion. This leads to the identification of a state equation relating the evolution of the relative Young's modulus to the damage ratio d/d_c where d represents the micro-cracks density and d_c a critical value identified using inverse engineering by introducing the experimental ultimate tensile stress values into the micromechanical model. The state equation is given by the following expression [18]:

$$\rho = \frac{d}{d_c} = \alpha\left[\left(\frac{E}{E_0}\right)\right]^2 + \beta\left[\left(\frac{E}{E_0}\right)\right] + \gamma \tag{11}$$

α, β and γ are micromechanical parameters depending on microstructure. Note that this equation is established and identified for the simple case of a tensile test. The assumption made in this study is that there is an intrinsic relationship between a local damage state and a macroscopic loss of stiffness also suitable under fatigue loading. On the other hand, the reduction of stiffness during a tensile test and during a fatigue test can be measured experimentally. Combining a linear expression of the tensile loss of stiffness to a power law expression of the fatigue loss of stiffness leads to the expression of the loss of stiffness under fatigue:

$$\frac{d}{d_c} = \alpha\left[\left(1 + a_i\left(\sigma^{imp} - \sigma_i^S\right)\right)\left\lfloor\frac{N}{22}\right\rfloor^{B_i}\right]^2 + \beta\left[\left(1 + a_i\left(\sigma^{imp} - \sigma_i^S\right)\right)\left\lfloor\frac{N}{22}\right\rfloor^{B_i}\right] + \gamma \tag{12}$$

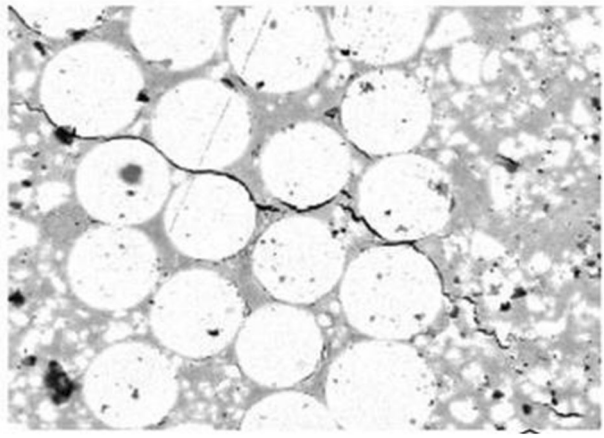

Fig. 7 Fiber-matrix interface decohesion as a main local damage mechanism in SMCs [29]

where σ^{imp} is the applied stress in fatigue, a_i and σ_i^S are the parameter defining the loss of stiffness under tensile loading and B_i represents the loss of stiffness kinetic under fatigue. The index, *i*, indicates the considered microstructure. From this expression, it is possible to plot the evolution of the local damage ration d/d_c under fatigue for several values of the applied stress versus the number of cycle (see Fig. 8). Finally, following this hybrid methodology allows converting the evolution of the macroscopic loss of stiffness to the evolution of a local damage indicator under fatigue.

One can note that this approach also allows fatigue life prediction by determining the number of cycles for which $d/d_c = 1$.

3.2 Pragmatic Adaptation Study on Peugeot 3008

This approach has been adapted for the design of the Peugeot 3008 tailgate. Structural simulation by FEM was performed and the stress distributions on the most critical areas (Fig. 3) introduced in Eq. (11) in order to analyse the damage cartography on these zones and validate the fatigue durability of this structural part.

4 New Reliability Approach

In order to solve the difficulty met in the application of the standard reliability method, the key idea in the proposed approach is the reconstruction of the distribution laws based on the Laribi &al. micromechanical based fatigue damage model. This damage model of the Peugeot 3008 tailgate structure was introduced in the Peugeot 3008 tailgate structure reliability validation. This chapter will present the principle of this new modular approach. One can note that the original idea proposed here can be adapted to any damage model.

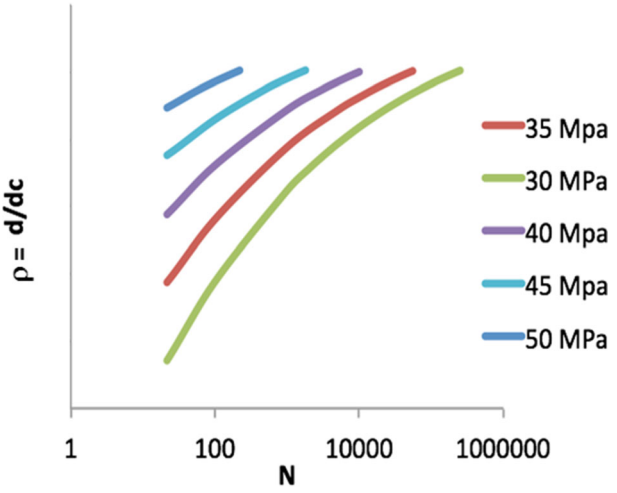

Fig. 8 Evolution of the local damage ratio for different values of the applied fatigue stress

4.1 Building of the Distributions in Damage Space

4.1.1 Definition of the Stress Distribution

The stress laws supplied by PSA [4] in term of LogNormal law for the number of cycles *(N)* and in term of Normal law for the slamming velocity *(V)* can be expressed analytically:

$$pr(N,V) = g(N) * Norm(V) \tag{13}$$

Where *pr(N,V)* is the probability to slam at *N* cycle with the velocity *V*. *g(N)* is the LogNormal law given in Eq. (1) and *Norm(V)* is the Normal distribution of the velocity given by the following equation:

$$Norm(V) = \frac{1}{\sigma\sqrt{2\pi}} e^{-\frac{1}{2}\left(\frac{V-\mu}{\sigma}\right)^2} \tag{14}$$

σ and μ are respectively the standard deviation and the mean. The 3D stress distribution illustrated in Fig. 9 meets all the mathematical properties of probability density:

- *pr(N,V)* is a continuous and differentiable function. Its integral form is obtained by the product of the integrals of the LogNormal and the Normal laws.
- The integral of *pr(N,V)* in the space *(N,V)* is obviously equal to *1*.

The stress density can be represented in a differential form as in Fig. 10.

As mentioned in the first chapter, the velocity can easily be transformed in term of stress (cf. Figure 4) using the following fourth-order polynomial:

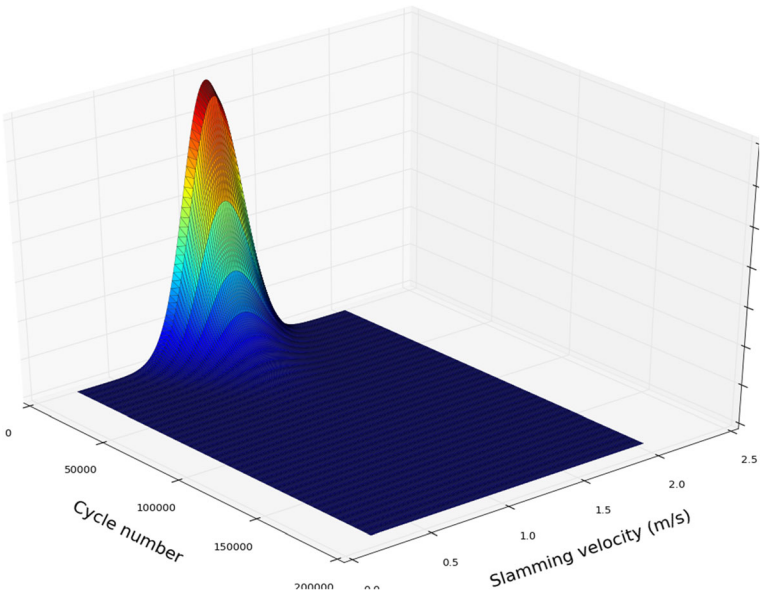

Fig. 9 Stress *pr(N,V)* 3D surface view

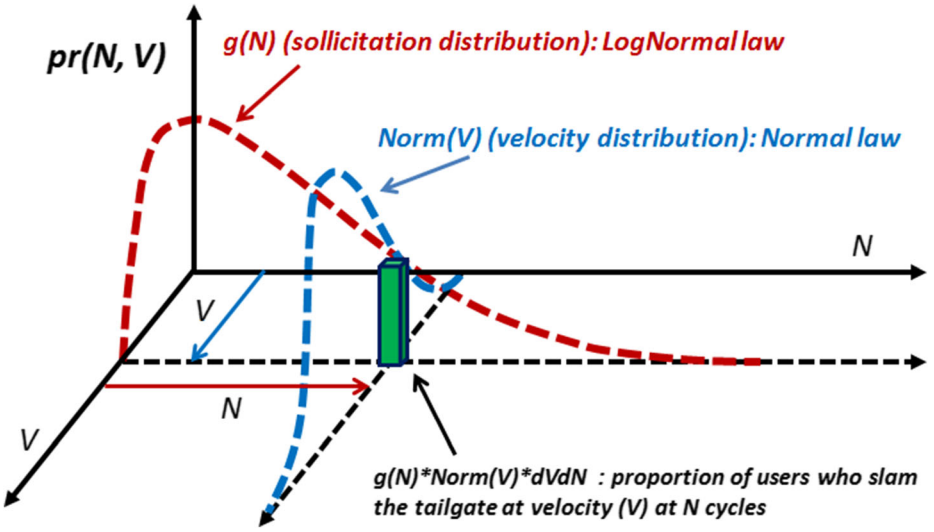

Fig. 10 Stress 3D view with velocity dispersion

$$\sigma\,(V) = a_1 V + a_2 V^2 + a_3 V^3 + a_4 V^4 \tag{15}$$

Where the $a_i (i = 1 \text{ to } 4)$ are the polynomial coefficients. This relation allows the integration of the damage model ρ in the analysis as the function of the tailgate slamming velocity and the cycle number N.

$$\rho = \frac{d}{dc} = \rho(N, \sigma(V)) \tag{16}$$

where $\sigma(V) = \sigma^{imp}$ of Eq. (12). The correlation between the event probability $pr(N,V)$ given by Eq. (13) and the damage level ρ occurred in the tailgate is clearly bi-univocal. The graphic illustration of damage evolution on the 3D surface is shown in Fig. 11:

From the expressions (13) and (16), a new density distribution based on damage can be defined by the following expressions:

$$\begin{cases} g(\rho) = \iint_{N=1,V=0}^{N_{max},V_{max}} LogNorm(N) * Norm(V) \\ \quad with\ \rho(N,V) = Constant \in [0, \rho_{max}] \end{cases} \tag{17}$$

The new density $g(\rho)$ is the sum of the initial densities $pr(N, V)$ for any couple (N,V) localized on the iso-values of damage. It takes automatically into account the velocity effect within its definition.

The density $g(\rho)$ has the advantage to be bounded in the damage space $[0, \rho_{max}]$ ρ_{max} is physically limited to a maximum value of 1corresponding to failure. However, to simplify the analytical development here, it can sometimes reach the value 1.2. The coherence of the results isn't affected.

4.1.2 Stress Density Building in Damage Space

To solve the Eqs. (17) and found the new distribution, in order to apply the stress-resistance method, a numerical approach is appropriate. To this aim, we have developed a Python algorithm where we calculate the proportion Dp of population which solicits the tailgate

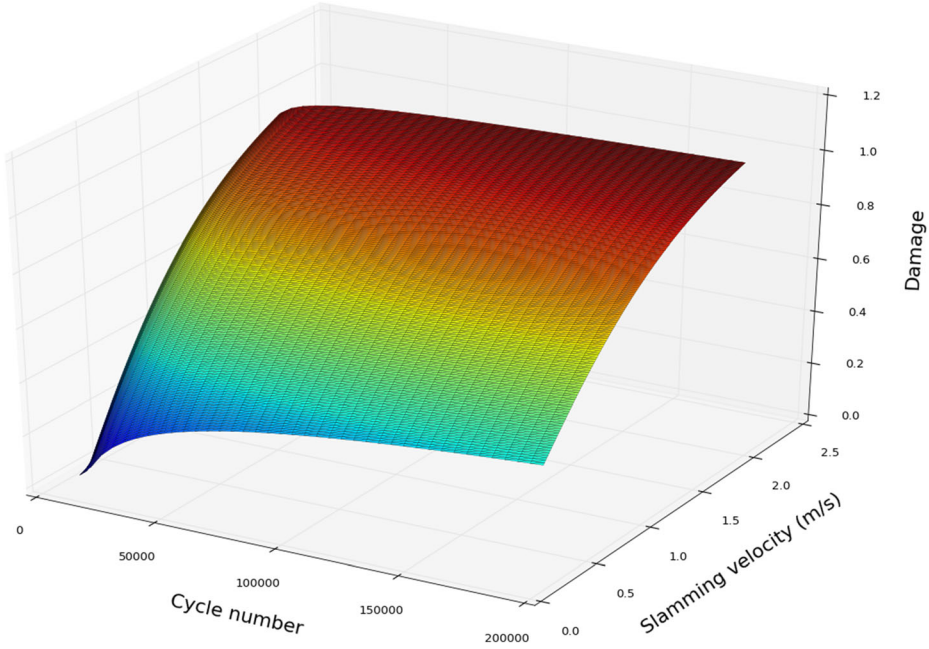

Fig. 11 Damage model in 3D representation

between the damage levels ρ and $\rho + d\rho$. Dp is given by the equations:

$$\begin{cases} Dp = L(\rho)g(\rho)d\rho \\ L(\rho) = \sum_{N=1,V=0}^{N_{max},V_{max}} \sqrt{dN^2 + dV^2} \\ d\rho = \dfrac{\partial\rho(N,V)}{\partial N}dN + \dfrac{\partial\rho(N,V)}{\partial V}dV \end{cases} \tag{18}$$

$L(\rho)$ represents the arc length of the isocline at the damage level ρ. The numerical resolution of these equations leads to the effective probability density $g(\rho)$ in damage dimension as it is illustrated on the following Fig. 12. It shows a very important effect of slamming velocity, non-advantageous for the ppm.

4.1.3 Definition of the Resistance Distribution

The building of the resistance density in damage space is simpler than the stress, since it is defined at a given reference velocity. From the expression of the Eq. (3), it is just a variable switching between the cycle number and the damage, at the reference velocity. We obtain:

$$f(\rho) = \frac{\beta}{\eta}\left(\frac{N(\rho)}{\eta}\right)^{\beta-1} e^{-\left(\frac{N(\rho)}{\eta}\right)^{\beta}} \frac{dN}{d\rho} \tag{19}$$

The damage model provides the relationship $N(\rho)$ between the cycle number and the damage. Thus defined, the resistance function has the same properties as a probability density. We can easily demonstrate that the cumulative sum in the damage space is equal to 1.

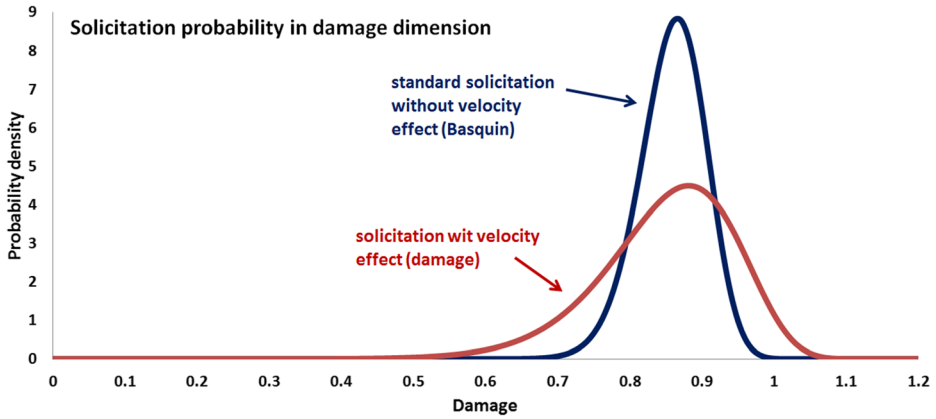

Fig. 12 Stress density in damage space

$$\int_0^{+\infty} f(N)dN = \int_0^{\rho_{max}} f(\rho)d\rho = 1 \tag{20}$$

4.2 Stress-Resistance in Damage Space

Once the distributions of stress and resistance reconstructions are completed, the application of stress-resistance is trivial. The Eqs. (5) and (6) expressed in damage space become:

$$\Delta(ppm) = [g(\rho_s)d\rho_s] * F(\rho_s) \tag{21}$$

$$ppm = \int_0^{\rho_{max}} [g(\rho_s)F(\rho_s)]d\rho_s \tag{22}$$

where $F(\rho)$ is the cumulative function of the density of resistance in damage space.

The iterative resolution of the Eq. (22) with the target ppm rate, leads to the final value of Eta (η) parameter. The result is presented in Fig. 13.

Finally, by assuming a Beta $\beta = 3.2$, the Eta parameter was calculated: $\eta = 3.e{+}6$ cycles. Following the same approach described in paragraph 2.3, the validation cycle number is calculated: $Ncycle = 2.e{+}6$ (normalized value). From this result an acceleration test about *35%* (factor *1.35*) from the reference velocity gives $N_{acc} = 450{,}000\ cycles$.

One can remark on the table below, the very huge gap between the results from the standard Basquin approach (without velocity effect) and new the damage approach. The damage approach is clearly realistic compared to the standard Basquin method (Table 1).

4.3 Damage Approach Consistency Analysis

In order to prove the consistency of the damage approach, with the analytical and numerical resolutions, we have performed two independent methods of solving. The next sections will briefly present and compare these approaches to the previous.

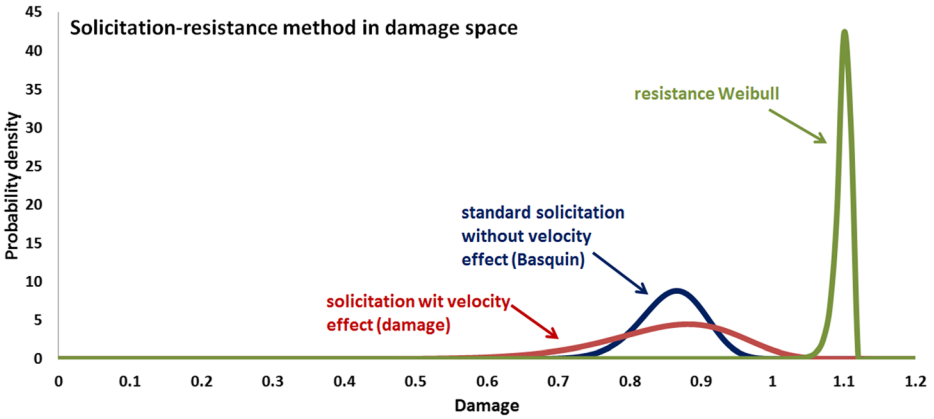

Fig. 13 Stress-resistance in damage space

4.3.1 Coming Back to N Cycle Dimension

From the effective density of the stress in damage space, it is easy to "come back" in *Ncycle* dimension. For a given damage value, the portion of population localized on the isocline is assigned to the corresponding cycle number at the reference velocity V_{ref}. This is achieved by the damage model $\rho = \rho(N, V_{ref})$. The resulting stress distribution in N dimension includes automatically the velocity effect. Figure 14 compares the result with the initial density in LogNormal law.

Since the Weibull resistance law is already expressed in N cycle dimension, the stress-resistance technic can be applied directly to identify the Eta η parameter. The results are rigorously the same than those obtained in the damage space: $\eta = 3.e{+}6$ and $Ncycle = 2.e{+}6$.

4.3.2 Resolution in 3D Space

From the effective distribution in damage space $g(\rho)$, it is also possible to reproduce a 3D distribution $pr(N, V)$. Therefore, it allows the 3D visualization of the effective distribution with the slamming velocity effect (Fig. 15).

Knowing the function $g(\rho)$, the inverse resolution of the Eqs. (17) leads to the 3D reproduction. The steps are:

- Relation between any point in space (N, V) and its corresponding damage level $\rho(N, V)$,
- Damage evaluation through the model,
- Density $g(N, V)$ calculation by inversion of the Eqs. (17)

Table 1 Damage approach vs Basquin method

Normed values	Standard Basquin method	Damage approach
η *(Weibull)*	4.e+5	3.e+6
Ncycles	2.4e+5	2.e+6
Nacc (factor 1.35)	2.2e-5	4.5e+5

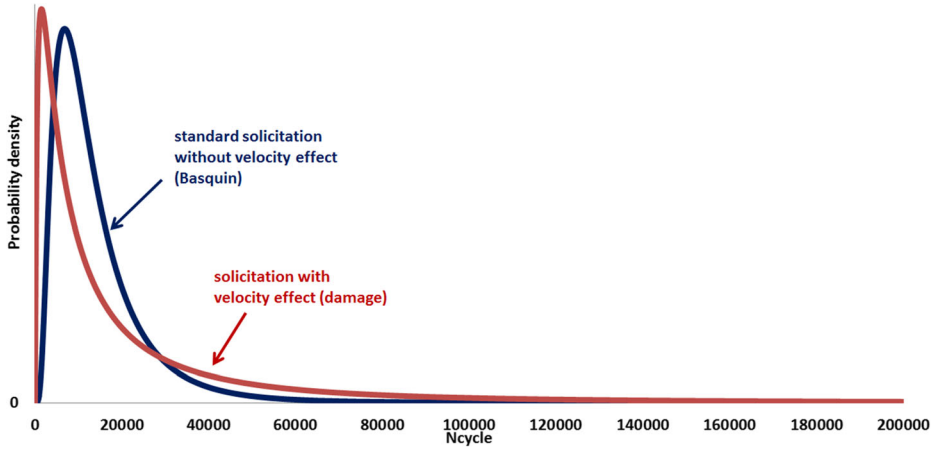

Fig. 14 Stresses (with and without velocity effect) in N space, from damage approach

Numerically, with a fine discretization in the *(N, V)* space, a linear interpolation may be sufficient to lead to a representative result. Figure 16 illustrates the differences between the obtained distribution *g(N, V)* and the standard density.

The 3D stress-resistance method is completed by the definition of the Weibull function in 3D. It is supposed to be constant with the slamming velocity. In that case, the 3D expression is the following.

$$f(N,V) = \left[\frac{\beta}{\eta}\left(\frac{N}{\eta}\right)^{\beta-1} e^{-\left(\frac{N}{\eta}\right)^{\beta}}\right] \frac{1}{V_{max} - V_{min}} \tag{23}$$

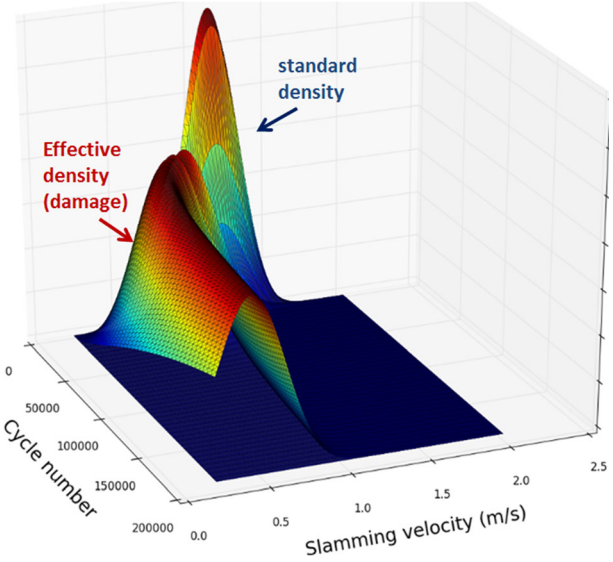

Fig. 15 Stress effective density in 3D view

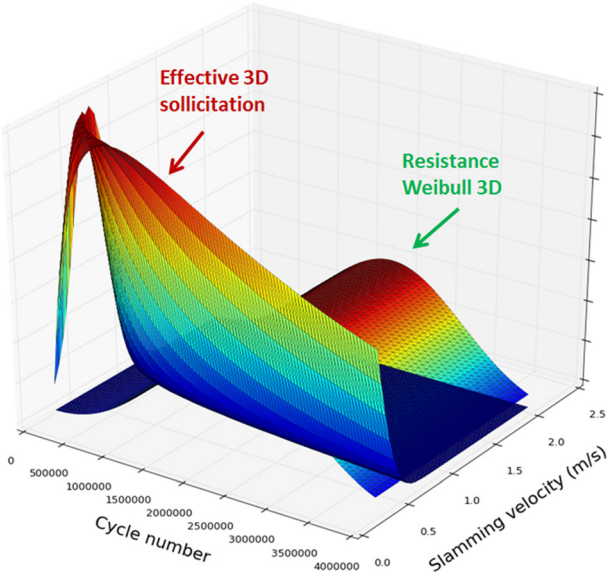

Fig. 16 Stress-resistance method in 3D

with V_{min} and V_{max}, respectively the minimum and the maximum slamming velocities. Its integral in the space *(N,V)* is equal to 1. Figure 16 gives its spatial representation, in combination with the effective density view.

The 3D form of the stress-resistance equation can be written as:

$$ppm = \iint_{N=1,V=Vmin}^{N=+\infty,V=V_{max}} [g(N,V)F(N,V)]dNdV \tag{24}$$

where *F(N,V)* is the 3D cumulative function of Weibull. The numerical resolution of the Eq. (24) leads to the values of Eta and the corresponding cycle number: $\eta = 2.95e{+}6$ and $Ncycle = 1.93e{+}6$. They are very close to the previous results. Finally, the entire approach consistency is clearly highlighted (Table 2) through the robustness of the results from three independent methods of resolution.

Table 2 Consistency of the damage approach

Normed values	Standard Basquin approach	Damage approach		
		Damage space 2D	*N* space 2D	*(N,V)* space 3D
η	4.e+5	3.e+6	3.e+6	2.95e+6
Ncycles	2.4e+5	2.e+6	2.e+6	1.93e+6
Nacc	2.2e-5	4.5e+5	4.5e+5	4.3e+5

5 Application on the New Peugeot 3008

In this section the new damage approach is applied to define the optimal test configuration to validate the target required by PSA on the tailgate of the new Peugeot 3008 (Fig. 17). By the way, the effect of doors opening or closing during the test is analysed. First of all, the state of damage with the given thermomechanical test imposed by PSA is evaluated using the micromechanical based fatigue damage law developed by Laribi & al [18].

5.1 Validation According to PSA Requirement

Figure 18 shows the profile of the thermomechanical fatigue loading requirement, according to PSA. This requirement comes from the metallic version of tailgate.

The cumulative damage state was calculated by the new model. It is represented on the following figure with the damage evolution for each temperature (Fig. 19).

These results indicate that damage occur and grow rapidly at the firsts dozens of cycles. However, it remain stable and failure is not observed, even if the damage value is high ($\rho = 96\%$). Although the physical test was accelerated, the failure was not observed. This is in good agreement with the model result. Nevertheless, there is no proof of product reliability. So, it is necessary to apply a rigorous approach from which the optimal validation test conditions can be found.

5.2 Optimal Test Conditions for the Tailgate Reliability

The presented reliability approach allows the definition of a reference state: $Ncycle = 2.e+6$ at the reference velocity V_{ref}. The corresponding damage level ρ_{ref} is the reference damage to be

Fig. 17 Durability test on tailgate 3008

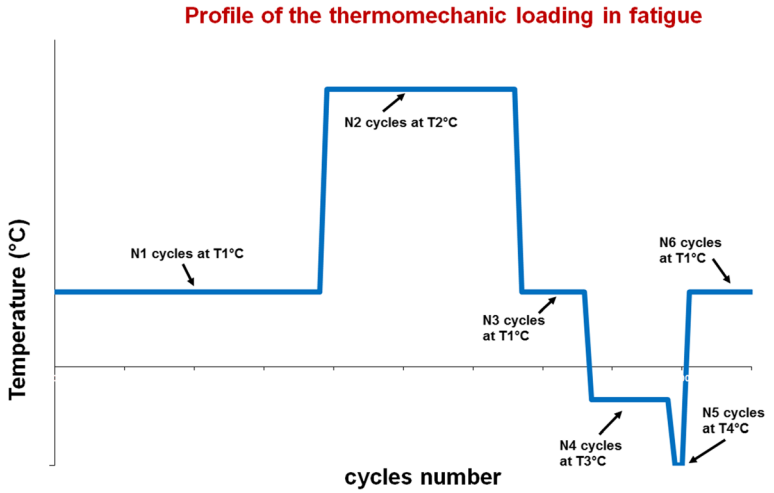

Fig. 18 PSA durability requirement on the tailgate

reached in any acceleration test. It represents the target iso-line in the space *(N, V)* illustrated in Fig. 20.

The acceleration is also possible with the temperature effect since the model provides the set of data from different applied temperatures. In order to reduce drastically the number of cycles it is recommended to combine temperature and velocity effects. The Table 3 below gives the results obtained by the damage approach. It highlights the strong acceleration effect. One can also note the reduction due to the doors closing. From the reference configuration, to the condition at 80 °C, doors closed and 36% of velocity acceleration, the required number of cycle to ensure reliability has been reduced more than 300 times. This final configuration is easier to be set-up in the laboratory to validate the ppm target.

The efficiency of the accelerated configuration is obvious. However, the robustness of these results is strongly link to the representativeness of the data: The given probability densities, the constitutive damage model and the FEM calculation.

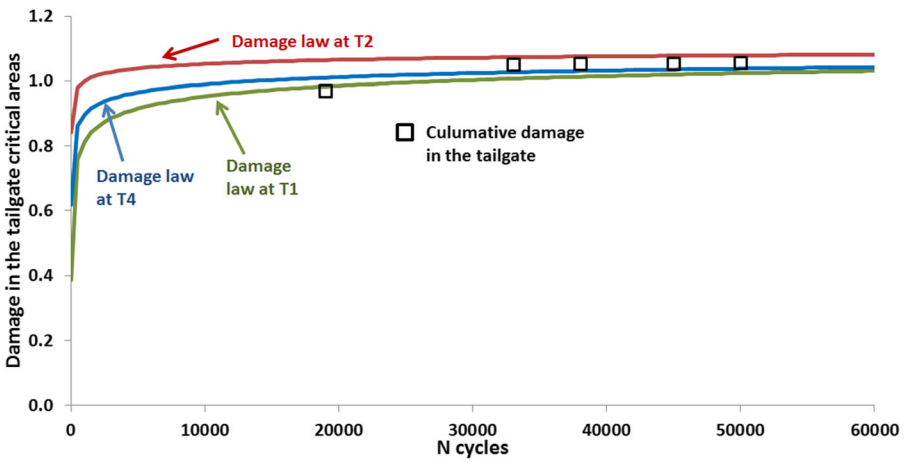

Fig. 19 State of cumulative damage (d/dc) on tailgate

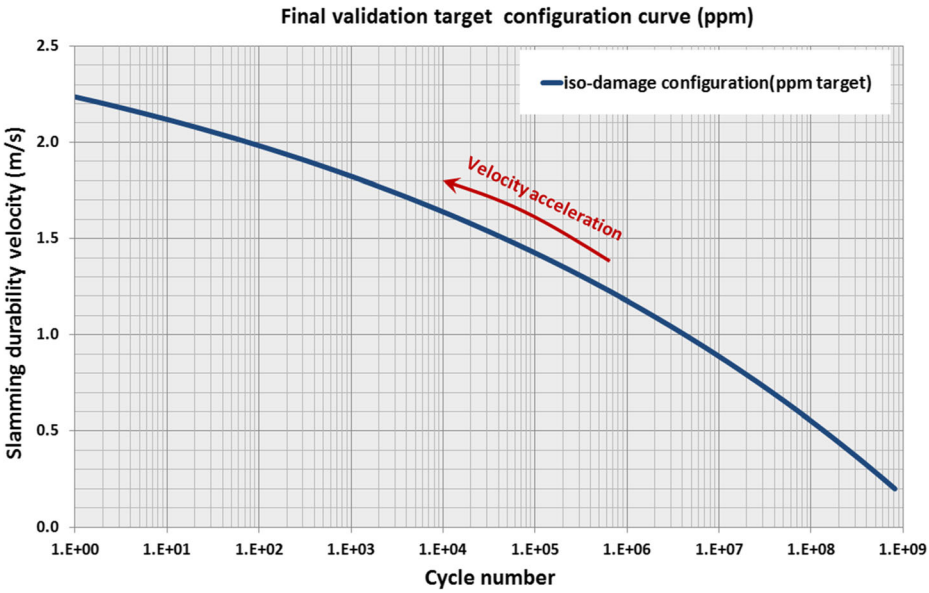

Fig. 20 ppm validation target line

Regarding the specific PSA tailgate, the confidence level was about 75%. This is a request imposed by the Original Equipment Manufacturer (OEM) to the supplier. With the proposed reliability approach, we showed in the Table 3 different reliable test configurations. Slamming test campaign has been set-up at the PSA test center. The purpose was to correlate the FEM model and to validate the global reliability approach. With different slamming velocities varying from 0,5 m/s to 2 m/s, the results have demonstrated the validity of the behavior curve in Fig. 20.

6 Conclusion

This paper has presented an original approach to ensure reliability of SMC material components. It has been applied to found the optimal configuration to validate the reliability of the manufactured Peugeot 3008 tailgate.

Table 3 Test configuration optimization for reliability

	$\theta°$	Velocity	Ncycle
Doors opened	21 °C	Vref	*2e+6*
	21 °C	36% of acc.	*4.5e+5*
	80 °C	Vref	*1.e+5*
	80 °C	36% of acc.	*2.e+4*
Doors closed	21 °C	Vref	*1.e+6*
probability = 75%	21 °C	36% acc	*6.e+4*
reduction factor = 30%	80 °C	Vref	*4e+5*
	80 °C	36% acc	*6e+3*

The current durability requirement of this tailgate is a direct adaptation of the metallic tailgates. But, the inadequacy of the standard Basquin method was demonstrated in the first part of the paper. Then, based to the established damage model, we have proposed a new approach. The key idea of this approach is the definition of a new stress probability in damage space, which advantageously takes into account the velocity effect, and is numerically bounded. Thus, the application of stress-resistance method leads to the resistance probability parameters. The consistency of the entire idea was demonstrated by the good correlation between three independents solving methods.

The application of this on the new Peugeot 3008 has allowed the definition of optimal laboratory test configurations, to validate the tailgate reliability. The stress and temperature accelerations contribute to reduce more than 300 times the number of cycle.

The robustness of this new damage approach is especially based on the predictive capacity of the micromechanical damage model which is based on a physical description close to reality. It also depends to the representativeness of the FEM model and the statistic laws. So, strong effort is on-going to refine the model.

On the other hand, deep investigations are also in-going to identify properly the statistic laws.

However, as this new approach is targeting practicing engineers in car industry, it is necessary to highlight the limitations of the method and how further studies, such as collecting more physical repeatable fatigue data, to correlate with the predictions and provide more confidence in the proposed design methodology.

Acknowledgments Authors address a strong acknowledgment to E. FEIGE and Y. HAMOY, from PSA, for the data provided. Their comments and advices were also very useful.

We are grateful to Mr. OZOUF for teaching and advices on the general topic of reliability.

References

1. Komeili, M., Milani, A.S.: The effect of meso-level uncertainties on the mechanical response of woven fabric composites under axial loading. Comput. Struct. **90–91**, 163–171 (2012). https://doi.org/10.1016/j.compstruc.2011.09.001
2. Zhu, T.: A reliability-based safety factor for aircraft composite structures. Comput. Struct. **48**(4), 745–748 (1993). https://doi.org/10.1016/0045-7949(93)90269-J
3. British Standards Institution BS 4994: 1987 Specification for design and construction of vessels and tanks in reinforced plastics; 1987
4. Papadopoulos, V., Papadrakakis, M.: Stochastic finite element-based reliability analysis of space frames. Probab. Eng. Mech. **13**(1), 53–65 (1998)
5. Philippidis, T.P., Lekou, D.J.: Probabilistic failure prediction for FRP composites. Compos. Sci. Technol. **58**(12), 1973–1982 (1998)
6. Gosling, P.D., Faimun, P.O.: A high-fidelity first-order reliability analysis for shear deformable laminated composite plates. Compos. Struct. **115**, 12–28 (2014)
7. Llorca, J., González, C., Molina-Aldareguía, J.M., Segurado, J., Seltzer, R., Sket, F., Rodríguez, M., Sádaba, S., Muñoz, R., Canal, L.P.: Multiscale modeling of composite materials: a roadmap towards virtual testing. Adv. Mater. **23**(44), 5130–5147 (2011)
8. Charmpis, D.C., Schuëller, G.I., Pellissetti, M.F.: The need for linking micromechanics of materials with stochastic finite elements: a challenge for materials science. Comput. Mater. Sci. **41**(1), 27–37 (2007)
9. G. Lamanna , A. Ceparano, L. Sartore. Reliability of Sheet Moulding Composites (SMC) for the Automotive Industry. Times of Polymers (TOP) and Composites 2014 AIP Conf. Proc. 1599, 338–341 (2014); https://doi.org/10.1063/1.4876847 © 2014 AIP Publishing LLC 978–0–7354-1233-0/$30.00

10. B. Hangs, D. Bücheler, M. Karcher, F. Henning, High-volume production of structural automobile parts: comparative study of relevant com
11. M. Bruderick, D. Denton, M. Shinedling, Applications of Carbon Fiber SMC for the Dodge Viper, Proceedings to Automotive Composites Conference & Exhibition (ACCE), Detroit (2013)
12. Jansen, C.: Isogrid-stiffened automotive suspension control arm. JEC Compos. Mag. **6**(82), 38 (2013)
13. M. Shirinbayan, J. Fitoussi, N. Abbasnezhad , F. Meraghni , B. Surowiec , A. Tcharkhtchi, Mechanical characterization of a Low Density Sheet Molding Compound (LD-SMC): Multi-scale damage analysis and strain rate effect. Composites Part B 131 (2017)
14. Bernasconi, A., Cosmi, F., Dreossi, D.: Local anisotropy analysis of injection moulded fibre reinforced polymer composites. Compos. Sci. Technol. **68**, 2574–2581 (2008)
15. L. Verger: "Exigences des CPPRs DCHM relatives à la Sûreté de Fonctionnement, Safety et Durabilité", PSA R&D direction, reference 01354_11_00248, pp. 1–19, January 30th 2012
16. P. Beaumont: "Optimisation des plans d'essais accélérés. Application à la tenue en fatigue de pieces métalliques de liason au sol", Chapter 4, pp. 61–98, PhD, February 5th 2014
17. B. Klimkeit: "Etude expérimentale et modélisation du comportement en fatigue multiaxiale d'un polymère renforcé pour application automobile", Chapter 6, pp. 105–146, PhD, december 3th 2009
18. Laribi, M.A., Tamboura, S., Fitoussi, J., Tié Bi, R., Tcharkhtchi, A., Dali, H.B.: Fast fatigue life prediction of short fiber reinforced composites using a new hybrid damage approach: application to SMC. Compos. Part B. **139**(15), 155–162 (2018). https://doi.org/10.1016/j.compositesb.2017.11.063
19. V. Ozouf: *Fiabilité des systèmes*, Partie N°5.3, pp. 96–109, Europe Qualité Services, EQS, Revision 3.2
20. J-C. Ligeron: Cours de fiabilité en mécanique, Chapter 3, pp. 81–82, IMdR M2OS, July 16th 2009
21. Fitoussi, J., Guo, G.B.D.: A statistical micromechanical model of anisotropic damage for S.M.C. composites. Compos. Sci. Technol. **58**, 759–763 (1998)
22. Tamboura, S., Sidhom, H., Baptiste, H., Fitoussi, J.: Evaluation de la tenue en fatigue du composite SMC R42. Mater. Tech. **89**, 3–4 (2001)
23. Fitoussi, J., Bourgeois, N., Guo, G., Baptiste, D.: Prediction of the anisotropic damaged behavior of composite materials: introduction of multilocal failure criteria in a micro-macro relationship. Comput. Mater. Sci. **5**(1), 87–100
24. Shirinbayan, M., Fitoussi, J., Meraghni, F., Surowieck, B., Laribi, M.A., Tcharkhtchi, A.: Coupled effect of loading frequency and amplitude on the fatigue behavior of advanced sheet molding compound (A-SMC). J. Reinf. Plast. Compos. (2016)
25. Jendli, Z., Meraghni, F., Fitoussi, J., Baptiste, D.: Multi-scales modelling of dynamic behaviour for discontinuous fibre SMC composites. Compos. Sci. Technol. **69**(1), 97–103 (2009)
26. Shirinbayan, M., Fitoussi, J., Meraghni, F., Surowiec, B., Bocquet, M., Tcharkhtchi, A.: High strain rate visco-damageable behavior of advanced sheet molding compound (A-SMC) under tension. Compos. Part B Eng. **82**, 30–41 (2015). https://doi.org/10.1016/j.compositesb.2015.07.010
27. Tamboura, S., Laribi, M.A., Fitoussi, J., Shirinbayan, M., Tie Bi, R., Tcharkhtchi, A., Ben Dali, H.: Damage and fatigue life prediction of short fiber reinforced composites submitted to variable temperature loading: application to sheet molding compound composites. Int. J. Fatigue. **138**, 105676 (2020)
28. Laribi, M.A., Tamboura, S., Fitoussi, J., Shirinbayan, M., Tie Bi, R., Tcharkhtchi, A., Ben Dali, H.: Microstructure dependent fatigue life prediction for short fibers reinforced composites: application to sheet molding compounds. Int. J. Fatigue. **138**, 105731 (2020)
29. Tamboura, S., Ayari, H., Shirinbayan, M., Laribi, M.-A., Bendaly, H., Sidhom, H., Tcharkhtchi, A., Fitoussi, J.: Experimental and numerical multi-scale approach for Sheet-Molding-Compound Composites fatigue prediction based on fiber-matrix interface cyclic damage. Int. J. Fatigue. **135**, 105526 (2020)

Affiliations

M. A. Laribi [1,2] · R. TieBi [3] · S. Tamboura [4] · M. Shirinbayan [1] · A. Tcharkhtchi [1] · H. Ben Dali [4] · J. Fitoussi [1]

R. TieBi
bob.valor-ext@faurecia.com

S. Tamboura
sahbi.tamboura@gmail.com

M. Shirinbayan
mohammadali.shirinbayan@ensam.eu

A. Tcharkhtchi
abbas.tcharkhtchi@ensam.eu

H. Ben Dali
hachmi.bdaly@gmail.com

J. Fitoussi
joseph.fitoussi@ensam.eu

[1] Institut Clément Ader ICA, CNRS UMR 5312, 3, Rue Caroline Aigle, 31400 Toulouse, France

[2] Arts et Metiers Institute of Technology, CNRS, CNAM, PIMM, HESAM University, F-75013 Paris, France

[3] Zero Emission, Faurecia Clean Mobility, Bois sur Prés, 25550 Bavans, France

[4] Ecole Nationale d'Ingénieurs de Sousse, LMS, Pôle technologique, 4054 Sousse, Tunisie